J. of Supercritical Fluids 54 (2010) 9–15

Contents lists available at ScienceDirect

The Journal of Supercritical Fluids

journal homepage: www.elsevier.com/locate/supflu

Theoretical study on interaction between CO_2 and carbonyl compounds: Influence of CO_2 on infrared spectroscopy and activity of C=O

Jinyao Wang[a,b,d], Meiyan Wang[c,d], Jianmin Hao[a,b,d], Shin-ichiro Fujita[e], Masahiko Arai[e], Zhijian Wu[c,*], Fengyu Zhao[a,b,**]

[a] State Key Laboratory of Electroanalytical Chemistry, Changchun Institute of Applied Chemistry, Chinese Academy of Sciences, Changchun 130022, PR China
[b] Laboratory of Green Chemistry and Process, Changchun Institute of Applied Chemistry, Chinese Academy of Sciences, Changchun 130022, PR China
[c] State Key Laboratory of Rare Earth Resource Utilization, Changchun Institute of Applied Chemistry, Chinese Academy of Sciences, Changchun 130022, PR China
[d] Graduate School, Chinese Academy of Sciences, Beijing 100049, PR China
[e] Division of Chemical Process Engineering, Graduate School of Engineering, Hokkaido University, Sapporo 060-8628, Japan

ARTICLE INFO

Article history:
Received 4 January 2010
Received in revised form 5 March 2010
Accepted 6 March 2010

Keywords:
Supercritical CO_2
Frequency shift
Local softness
Hydrogenation

ABSTRACT

The interactions between CO_2 and carbonyl compounds at different CO_2 pressures have been studied both experimentally and theoretically. In situ high-pressure FTIR on carbonyl compounds, i.e., acetaldehyde, acetone, and crotonaldehyde, in supercritical CO_2 have been measured at various CO_2 pressures varying from 6 to 22 MPa. In order to get insights into the mechanism, theoretical study has been conducted concerning the effect of CO_2 on frequency shift of C=O in acetaldehyde, acetone, benzaldehyde, crotonaldehyde and cinnamaldehyde at different CO_2 pressures. It has been shown that the experimental frequency shifts can be well simulated by the theoretical model calculations using particular structures, in which a carbonyl compound interacts with a few CO_2 molecules, depending on the carbonyl compounds examined, except for acetaldehyde.

The interaction energies between CO_2 and those carbonyl compounds are also given. In addition, the effect of CO_2 on hydrogenation of crotonaldehyde and benzaldehyde has been discussed by means of the local softness (s^+) calculated at CO_2 pressures of 0–22 MPa, which can explain the reactivity difference in the crotonaldehyde and benzaldehyde hydrogenations in supercritical CO_2.

1. Introduction

Supercritical carbon dioxide ($scCO_2$) has shown great potential as a replacement for conventional organic solvents. $ScCO_2$ is readily available (T_c = 31.1 °C and P_c = 7.4 MPa), inexpensive, nontoxic, nonflammable and its density and diffusion coefficient can be tuned by the change of the pressure and the temperature [1–3]. Therefore, the use of $scCO_2$ has been attracting more and more attention for developing green chemical processes. Hydrogenation is one of the most studied reactions in $scCO_2$, in which the reaction rate and product selectivity could be improved significantly [4–16]. In most studies reported so far, it is thought that the enhancement of rate of catalytic hydrogenation in $scCO_2$ is from the higher H_2 concentration or the lower mass transfer resistance [16–21]. In our previous work, the molecular interaction between CO_2 and cinnamaldehyde was investigated by using high-pressure FTIR, and a red-shift of carbonyl group C=O vibration was observed in compressed CO_2, suggesting that there exists a molecular interaction between CO_2 and cinnamaldehyde [5,11]. The specific interaction between CO_2 and solutes has been also theoretically studied by several groups [22,23]. Borkman and co-worker have investigated the CO_2 binding to carbonyl groups using *ab initio* method and suggested that the specific interaction between CO_2 and carbonyl oxygen is the Lewis acid–base interaction [22]. Raveendran and co-workers indicated that the Lewis acid–base interaction between the carbon atom of CO_2 and carbonyl oxygen is accompanied by a cooperative intermolecular C–H···O interaction between the oxygen in CO_2 and hydrogen atom attached to the carbonyl carbon or at the α-position [23]. However, the strength of interaction which affects the reactivity of carbonyl groups in $scCO_2$ medium has not been systematically studied.

The theoretical study combined with the vibrational spectroscopy is a very useful tool for investigating the solvent–solute interaction. Besnard and co-workers have studied the CO_2–ethanol interaction by both theoretical study and the experimental infrared spectroscopy and found that the attractive interactions played a

* Corresponding author. Tel.: +86 0431 85262801; fax: +86 0431 85698041.
** Corresponding author at: State Key Laboratory of Electroanalytical Chemistry, Changchun Institute of Applied Chemistry, Chinese Academy of Sciences, 5625 Renmin Street, Changchun 130022, Jilin, PR China. Tel.: +86 0431 85262410; fax: +86 0431 85262410.
E-mail addresses: zjwu@ciac.jl.cn (Z. Wu), zhaofy@ciac.jl.cn (F. Zhao).

0896-8446/$ – see front matter © 2010 Elsevier B.V. All rights reserved.
doi:10.1016/j.supflu.2010.03.002

dominant role in stabilizing the energy between CO_2 and ethanol [24]. Cappelli et al. have calculated the OH stretch in liquid water and methanol by the cluster–continuum model and studied the effects of the parameters of continuum models on the vibrations [25].

In this paper, we first reported experimental infrared spectra of acetaldehyde, acetone, benzaldehyde, crotonaldehyde and cinnamaldehyde diluted in $scCO_2$, then the molecular interactions between CO_2 and the carbonyl group of these carbonyl compounds in $scCO_2$, which were studied by density functional method through examining the infrared vibrational frequencies of carbonyl group. Finally, the effect of $scCO_2$ on hydrogenation of carbonyl compounds was also investigated by the local softness.

2. Experimental details

In situ high-pressure FTIR spectra of acetaldehyde, acetone, and crotonaldehyde were measured at 50 °C with an FTIR spectrometer (FT/IR-620, JASCO) as described in our previous work [11]. A 1.5 cm^3 high-pressure cell with a path length of 4 mm was used. 10 μL substrate was added to the cell and was heated to 50 °C by the circulation of preheated oil outside the cell, and then CO_2 was introduced into the cell. The pressure was raised slowly while stirring by a Teflon-coated magnetic stirrer. When the pressure reached the desired value, the stirring was further continued for 3–5 min and stopped; then the IR spectra were measured with a triglycine sulfate (TGS) detector at 4 cm^{-1} wavenumber resolution. In this measurement, the concentration of the carbonyl compounds dissolved is different and depends on the solubility of them in CO_2. A fraction of 10 μL sample was soluble in CO_2 and FTIR was measured for the gas mixture of the dissolved carbonyl compound and CO_2. The amount of substrates added has no effect on the peak positions of the absorption bands.

3. Computational methods

The calculations were performed using the Gaussian 03 suite of programs [26]. The proposed geometries were first optimized at the gas phase at B3LYP level with 6-311+G(d,p) basis set [27–29]. Frequency calculations have been carried out at the same level. The obtained geometries were reoptimized by solvent model. Since the combination of the CO_2 molecule with model carbonyl compounds gives many possible conformers, only the conformer with the lowest energy in the gas phase was chosen for the further study in solution. The single point energies at these optimized complexes were calculated at MP2/6-31+G* level. The interaction energies of the complexes were calculated using the "supermolecule" model (described below) as the difference in energy between the each complex and the sum of the isolated monomers. The interaction energies were corrected for the basis set superposition errors (BSSE) using the full counterpoise method of Boys and Bernardi [30].

In polarizable continuum model (PCM), the solvent is treated as a dielectric continuous medium. The solute is placed inside a spherical or ellipsoidal cavity in the dielectric continuous medium but the drawback of the model is the neglect of the short-range specific solute–solvent interaction [31–33]. In the supermolecule model, a solvation system is modeled by a molecular complex of the solute with a small number of solvent molecules in vacuum and the specific solute–solvent interaction is modeled by the complex, but the model disregards the long-range solute–solvent interaction [34]. In order to better simulate the solvent effect, the cluster–continuum model is proposed by Riveros and co-worker [35]. The method considers the solvent as a dielectric continuum and the solute as a supermolecule imbedded in a cavity in the continuum, which takes into account of both long-range solute–solvent interaction and the short-range specific solute–solvent interaction. In this work, the bulk solvent CO_2 molecules were represented by the dielectric constant, density and radius of the CO_2 molecule in polarizable continuum model. We optimized the complex structure by PCM with using the parameters like dielectric constant and density of CO_2 at the experimental temperature and pressure, for which these parameters could respond the property of CO_2 at different pressures. The dielectric constant and density at different CO_2 pressures were obtained from the literature [36]. The radius of the CO_2 molecule is 1.824 Å [37].

After the optimization considering solvent effect, frequency calculations were carried out and the atomic charges were evaluated by using the natural bond orbital (NBO) analysis [38].

As the atomic charges were available, the local softness can be obtained by using the following formulas. In density functional theory (DFT), the global hardness (η) [38–40] is defined as

$$\eta = \frac{1}{2}\left(\frac{\partial^2 E}{\partial N^2}\right)_{\nu(\vec{r})} = \frac{1}{2}\left(\frac{\partial \mu}{\partial N}\right)_{\nu(\vec{r})} \tag{1}$$

where E, N, μ, and $\nu(\vec{r})$ are the energy, number of electrons, chemical potential and external potential, respectively.

The global softness, S, is defined as

$$S = \frac{1}{2\eta} = \left(\frac{\partial N}{\partial \mu}\right)_{\nu(\vec{r})} \tag{2}$$

Using the finite difference approximation, S can be approximated as

$$S = \frac{1}{IE - EA} \tag{3}$$

where IE and EA are the first ionization energy and electron affinity of the molecule, respectively.

The local property, Fukui function [41] $f(\vec{r})$ is defined as the derivative of electron density, $\rho(\vec{r})$, with respect to the number of electrons at a constant external potential, $\nu(\vec{r})$

$$f(\vec{r}) = \left(\frac{\partial \rho(\vec{r})}{\partial N}\right)_{\nu(\vec{r})} \tag{4}$$

Applying the finite difference approximation, the condensed Fukui function of an atom, say k, in a molecule with N electrons is defined as

$$\begin{aligned} f_k^+(\vec{r}) &= q_k(N+1) - q_k(N), \quad \text{governing the nucleophilic attack on the system} \\ f_k^-(\vec{r}) &= q_k(N) - q_k(N-1), \quad \text{governing the electrophilic attack on the system} \\ f_k^0(\vec{r}) &= [q_k(N+1) - q_k(N-1)]/2, \quad \text{governing the radical attack on the system} \end{aligned} \tag{5}$$

where $q_k(N)$, $q_k(N+1)$ and $q_k(N-1)$ are atomic charges for atom k in the N, $(N+1)$ and $(N-1)$-electron systems.

Similarly, local softness [42], $s(\vec{r})$, is defined as the derivative of electron density, $\rho(\vec{r})$, with respect to the chemical potential, μ, at a constant external potential,

$$s(\vec{r}) = \left(\frac{\partial \rho(\vec{r})}{\partial \mu}\right)_{\nu(\vec{r})} = \left(\frac{\partial \rho(\vec{r})}{\partial N}\right)_{\nu(\vec{r})} \cdot \left(\frac{\partial N}{\partial \mu}\right)_{\nu(\vec{r})} = f(\vec{r}) \cdot S \tag{6}$$

Atomic softness values can be calculated by

$$\begin{aligned} s_k^+(\vec{r}) &= [q_k(N+1) - q_k(N)]S \\ s_k^-(\vec{r}) &= [q_k(N) - q_k(N-1)]S \\ s_k^0(\vec{r}) &= S[q_k(N+1) - q_k(N-1)]/2 \end{aligned} \tag{7}$$

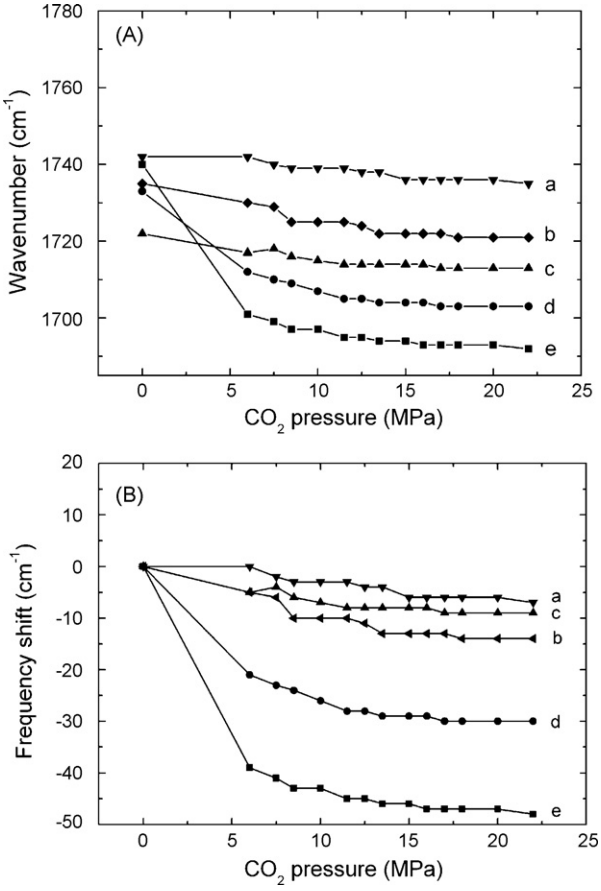

Fig. 1. (A) Peak position of C=O absorption band as a function of CO_2 pressure at $T = 50\,^{\circ}C$ and (B) C=O vibrational frequency shift at different CO_2 pressures. a: acetaldehyde, b: acetone, c: benzaldehyde, d: crotonaldehyde, and e: cinnamaldehyde. Infrared spectra of cinnamaldehyde and benzaldehyde were reported in Ref. [11].

Atomic softness for crotonaldehyde and benzaldehyde in ambient gas phase and at different CO_2 pressures are calculated using Eq. (7).

4. Results and discussion

4.1. Experimental infrared spectra of carbonyl compounds diluted in scCO$_2$

The specific interaction between CO_2 and carbonyl groups has been examined experimentally by using the IR spectroscopy [43]. In this study, the in situ high-pressure FTIR was measured for the C=O vibrational frequency of acetaldehyde, acetone and crotonaldehyde at the CO_2 pressure range of 0–22 MPa (Fig. 1A). For comparison, the data of benzaldehyde and cinnamaldehyde published in the previous study [11] is also given in Fig. 1. It is noted that the C=O vibrational frequencies of all carbonyl compounds decrease with the increase of pressure, and the red-shift is larger for cinnamaldehyde and crotonaldehyde compared with the others. In order to study the frequency shifts of the C=O, we plotted the frequency shifts as a function of pressure (Fig. 1B). The frequency shifts of C=O bond in carbonyl compounds were determined by comparing the values at different CO_2 pressures with that in vacuum. It is observed that the frequency shifts of cinnamaldehyde and crotonaldehyde are up to 48 cm^{-1} and 30 cm^{-1}, but the frequency shift of benzaldehyde, acetone and acetaldehyde is only 9 cm^{-1}, 14 cm^{-1} and 7 cm^{-1}, respectively, which means that the frequency shift of C=O depends strongly on the configuration of the carbonyl compounds. Because

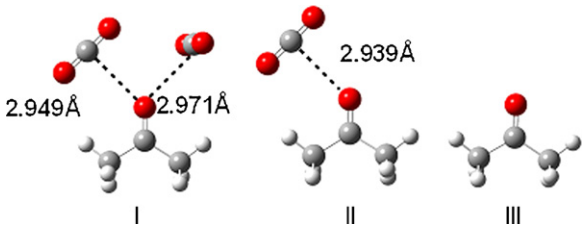

Fig. 2. Optimized geometries for the complex acetone–$(CO_2)_n$ ($n = 0, 1, 2$) at CO_2 pressure of 18 MPa.

of the conjugated "π" bond between ethylene and carbonyl group, crotonaldehyde and cinnamaldehyde have higher frequency shift. While the other model compounds without such conjugated "π" bonds showed a smaller frequency shift. Meanwhile, the C=O vibrational frequency shifts have nonlinear decrease with the increase of pressure (Fig. 1B). The nonlinear behavior of the shift may be related to the local density enhancements around the attractive solutes in solutions, which has been well studied and confirmed by the computer simulation studies [44,45].

4.2. Theoretical calculation of vibrational frequencies

In order to gain further insights into effect of CO_2 on the frequency shift of C=O, we carried out the quantum chemical calculations. For each solute molecule, such as acetone, different numbers of CO_2 have been considered to interact with the molecule. The conformers obtained from the combination of CO_2 and each solute molecule were optimized at different pressures. The results indicate that for each conformer, the optimized geometries are different at different pressures, which results in a difference in the vibrational frequency. In this work, only the geometries at 18 MPa are shown and the others in the supporting information.

4.2.1. Interaction between acetone and CO$_2$

The carbon atom in CO_2 molecule has positive charges that can attract negative charges and acts as Lewis acid. The oxygen in acetone has two lone electron pairs and acts as Lewis base. The existence of Lewis acid–base interaction between CO_2 and acetone was reported in the literature [46]. Possible geometries of the supermolecule acetone–$(CO_2)_n$ ($n = 0, 1, 2$) are displayed in Fig. 2. The obtained vibrational frequency shifts together with experiment data are listed in Table 1. The agreement between the experimental and calculated results are found for the conformer I with two CO_2 molecules, i.e., acetone–$(CO_2)_2$, except for the value at 6 MPa. At 6 MPa, the conformer II acetone–CO_2 gives a vibrational frequency shift −7.16 cm^{-1}, close to the experimental value −5 cm^{-1}. Recently, Besnard et al. measured Raman spectra of the CO_2 complex in CO_2 and acetone mixtures, and they found a new band at about 655 cm^{-1} which was attributed to the formation of a 1:1 electronic donor acceptor acetone–CO_2 complex

Table 1
Calculated and experimental C=O vibrational frequency shift of acetone at different CO_2 pressures for conformers I (acetone–$(CO_2)_2$), II (acetone–CO_2) and III (acetone).

Pressure (MPa)	Exp. shift (cm^{-1})	Calc. shift (cm^{-1})		
		I	II	III
6	−5	−10.73	−7.16	−0.23
8.5	−10	−10.81	−7.31	−1.81
10	−10	−10.90	−9.26	−2.74
16	−13	−13.27	−10.88	−4.93
18	−14	−13.39	−11.05	−5.15
20	−14	−14.71	−11.17	−5.32
22	−14	−14.81	−11.27	−5.45

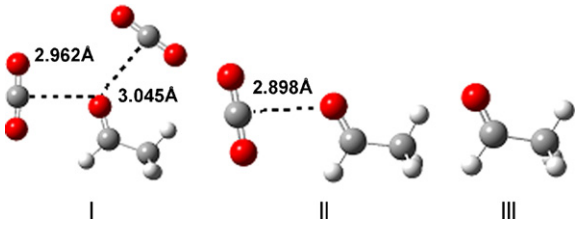

Fig. 3. Optimized geometries for the complex acetaldehyde–$(CO_2)_n$ (n = 0, 1, 2) at CO_2 pressure of 18 MPa.

at a pressure of 8 MPa [47]. These are in agreement to the present results that the acetone–CO_2 complex was formed at 6 MPa and the acetone–$(CO_2)_2$ complex is formed at pressures above 8.5 MPa. This may be related to the compressibility of $scCO_2$, in which the density changes with CO_2 pressures. At lower pressure, the complex of one CO_2 molecule interacting with one acetone is preferred, while at high pressures, the complex of two CO_2 molecules interacting with one acetone is preferred. While considering only the acetone molecule itself (conformer III in Fig. 2) using the PCM, the calculated values are much smaller compared with the experiment data (Table 1). This demonstrates that the cluster–continuum model, which considers the solvent molecules explicitly, can better simulate the frequency shifts of C=O of acetone at different CO_2 pressures and the short-range interaction between CO_2 and acetone is very important for frequency shift of C=O of acetone.

4.2.2. Interaction between acetaldehyde and CO_2

Fig. 3 shows the optimized geometries of the acetaldehyde–$(CO_2)_n$ (n = 0, 1, 2). The shifts of C=O vibrational frequencies at different CO_2 pressures are compared with the experimental data and listed in Table 2. The calculated results show that the frequency shifts based on the geometry of acetaldehyde molecule itself using PCM (i.e., without interacting with CO_2), give much closer data compared with the experimental values (Table 2). For conformers I and II, the relatively larger vibrational frequency shifts are obtained compared to the experimental data. This suggests that the interaction between CO_2 and acetaldehyde is very week. In addition, the dimer of acetaldehyde in $scCO_2$ was also considered in this work, but the calculated results show that the frequency shift of the dimer was quite small compared with the values of experiment and monomer, indicating the dimer is not possible under the present conditions.

4.2.3. Interaction between benzaldehyde and CO_2

The optimized geometries are displayed in Fig. 4. For the conformer I, the calculated frequency shifts are much larger than experimental data (Table 3). For the interaction with one CO_2 molecule, two interesting conformers (II and III) were obtained. The difference between the two conformers is the orientation of CO_2 molecules. It is interesting to note that the frequency shifts based on the conformer III are much close to the experimental data at the pressures examined (Table 3). In this complex, the CO_2 molecule is almost vertical to the benzaldehyde molecular plane which may be due to the steric repulsion of aromatic. While, with the conformer II, the vibrational frequency shifts is overestimated, in which the CO_2 molecule is in the benzaldehyde molecular plane. For the molecule benzaldehyde itself (conformer IV) in PCM model, underestimation is observed, in particular at the lower pressures. This suggests that in searching the possible conformers, one has to try the possible orientations of the CO_2 molecule(s) in the initial geometry, which is the strategy of our calculation. Our results also reveal that the cluster–continuum model can better simulate the frequency shifts of C=O of benzaldehyde at different CO_2 pressures in which one CO_2 molecule interacts with one benzaldehyde is preferred.

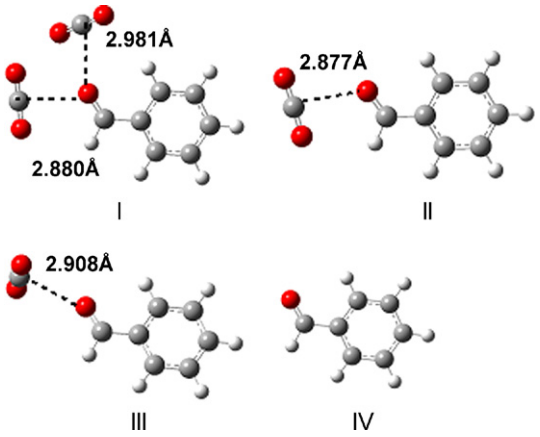

Fig. 4. Optimized geometries for the complex benzaldehyde–$(CO_2)_n$ (n = 0, 1, 2) at CO_2 pressure of 18 MPa.

4.2.4. Interaction between crotonaldehyde and CO_2

In crotonaldehyde, there exists the conjugated "π" bond between C=C and carbonyl group. Therefore, we may expect that the intermolecular interaction should be strong between crotonaldehyde and CO_2 molecule. This can indeed be seen from our results (Fig. 5 and Table 4). From Table 4, it is noted that at 6 MPa, the crotonaldehyde–$(CO_2)_2$ (conformer III in Fig. 5) gives the frequency shift $-19.54\,cm^{-1}$, close to the experimental value $-21\,cm^{-1}$. The differences from the other two conformers (I and II) are slightly larger. At 8.5 MPa, crotonaldehyde–$(CO_2)_3$ (conformer II) gives the best agreement with the experimental data. At 10 MPa, the results from crotonaldehyde–$(CO_2)_3$ ($-25.18\,cm^{-1}$) and crotonaldehyde–$(CO_2)_4$ ($-27.88\,cm^{-1}$) (conformer I) are competitive compared with the experimental value ($-26.00\,cm^{-1}$), but the former is preferred slightly. From 16 to 22 MPa, the results from crotonaldehyde–$(CO_2)_4$ are clearly better than the other conformers. Meanwhile, it is also noted that with the increase of pressure more and more CO_2 molecules take part in the interac-

Table 2
Calculated and experimental C=O vibrational frequency shifts of acetaldehyde at different CO_2 pressures for conformers I (acetaldehyde–$(CO_2)_2$), II (acetaldehyde–CO_2) and III (acetaldehyde).

Pressure (MPa)	Exp. shift (cm^{-1})	Calc. shift (cm^{-1})		
		I	II	III
6	−0	−17.82	−10.63	−0.34
8.5	−3	−17.94	−10.77	−2.30
10	−3	−18.08	−10.94	−3.37
16	−6	−18.42	−14.12	−5.87
18	−6	−18.45	−14.35	−6.12
20	−6	−18.48	−14.53	−6.31
22	−7	−18.50	−14.66	−6.46

Table 3
Calculated and experimental C=O vibrational frequency shifts of benzaldehyde at different CO_2 pressures for conformers I (benzaldehyde–$(CO_2)_2$), II (benzaldehyde–CO_2), III (benzaldehyde–CO_2) and IV (benzaldehyde).

Pressure (MPa)	Exp. shift (cm^{-1})	Calc. shift (cm^{-1})			
		I	II	III	IV
6	−5	−15.09	−11.34	−4.80	−1.48
8	−6	−15.24	−11.57	−5.70	−2.54
10	−7	−15.41	−13.50	−6.59	−3.72
16	−8	−20.65	−16.08	−9.87	−7.21
18	−9	−20.84	−16.53	−10.12	−7.52
20	−9	−20.98	−16.74	−10.31	−7.77
22	−9	−21.09	−16.88	−10.46	−7.96

Table 4
Calculated and experimental C=O vibrational frequency shifts of crotonaldehyde at different CO_2 pressures for conformers I (crotonaldehyde–$(CO_2)_4$), II (crotonaldehyde–$(CO_2)_3$), III (crotonaldehyde–$(CO_2)_2$), IV (crotonaldehyde–CO_2) and V (crotonaldehyde).

Pressure (MPa)	Exp. shift (cm^{-1})	Calc. shift (cm^{-1})				
		I	II	III	IV	V
6	−21	−27.36	−24.67	−19.54	−10.04	−0.40
8	−24	−27.61	−24.91	−19.75	−12.06	−2.62
10	−26	−27.88	−25.18	−19.98	−13.12	−4.04
16	−29	−30.00	−27.87	−24.11	−17.59	−9.79
18	−30	−30.14	−28.02	−24.33	−17.97	−10.22
20	−30	−30.24	−28.14	−24.5	−18.28	−10.54
22	−30	−30.32	−28.23	−24.65	−18.51	−10.80

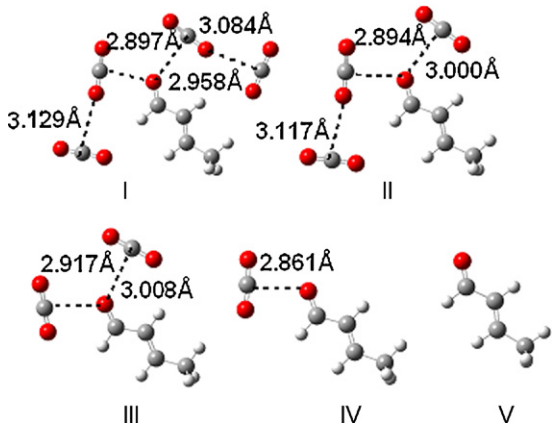

Fig. 5. Optimized geometries for the complex crotonaldehyde–$(CO_2)_n$ (n = 0, 1, 2, 3, 4) at CO_2 pressure of 18 MPa.

tion with crotonaldehyde. At the pressure range of 16–22 MPa, the CO_2 molecules in the first solvation shell of C=O of crotonaldehyde are saturated and so the frequency shift has no change. Our results demonstrate that the explicit inclusion of the solvent molecules in the cluster–continuum model can better simulate the frequency shifts of C=O of crotonaldehyde at different CO_2 pressures, and with the increase of pressure, more CO_2 molecules accumulate around C=O of crotonaldehyde.

4.2.5. Interaction between cinnamaldehyde and CO_2

Based on the above studies the geometries of crotonaldehyde and benzaldehyde containing conjugated "π" bonds, herein, a larger molecule of cinnamaldehyde with both the "π" of benzene ring and ethylene, which conjugates with carbonyl group, was studied also. The results show that cinnamaldehyde–$(CO_2)_4$ (conformer I) gives better result compared with the other conformers (Table 5 and Fig. 6). Meanwhile, with the increase of pressure from 6 to 22 MPa, the calculated vibrational frequency shifts in cinnamaldehyde–$(CO_2)_4$ changes slightly from $-30.05\,cm^{-1}$ to $-32.16\,cm^{-1}$, which are smaller than the experimental data, indicating more CO_2 molecules would interact with cinnamaldehyde. However, the present method was unable to make the calculation with more than 4 CO_2 molecules.

Table 5
Calculated and experimental C=O vibrational frequency shifts of cinnamaldehyde at different CO_2 pressures for conformers I (cinnamaldehyde–$(CO_2)_4$), II (cinnamaldehyde–$(CO_2)_3$), III (cinnamaldehyde–$(CO_2)_2$), IV (cinnamaldehyde–CO_2), and V (cinnamaldehyde).

Pressure (MPa)	Exp. shift (cm^{-1})	Calc. shift (cm^{-1})				
		I	II	III	IV	V
6	−39	−30.05	−26.27	−22.04	−11.58	−0.43
8	−43	−30.23	−26.49	−23.64	−13.39	−2.94
10	−43	−30.49	−28.01	−25.53	−14.52	−4.44
16	−47	−31.82	−29.51	−27.45	−19.08	−10.66
18	−47	−31.96	−29.66	−28.67	−19.43	−11.11
20	−47	−32.06	−29.78	−28.89	−19.71	−11.46
22	−48	−32.16	−29.87	−29.06	−19.91	−11.74

4.3. Analysis of molecular interactions from the charge transfer, bond length change and interaction energies

It was reported that the carbonyl groups in unsaturated aldehydes of crotonaldehyde and cinnamaldehyde were much easier to be hydrogenated and the selectivity to the corresponding unsaturated alcohols was enhanced significantly in $scCO_2$ [11]. This was suggested from the molecular interactions between the reactant and CO_2 molecules. Based on our above results and discussion, the cluster–continuum model can be better simulate $scCO_2$ solvent effect on frequency shifts of C=O bond in the carbonyl compounds studied in this work, except for acetaldehyde. Thus, the intermolecular interaction energies (ΔE_{cor}) at a CO_2 pressure of 18 MPa are calculated (Table 6). The results show that the molecular interaction energies (ΔE_{cor}) are in the following order: acetaldehyde < benzaldehyde < acetone < crotonaldehyde < cinnamaldehyde. It is clear that stronger interaction exists between CO_2 and unsaturated carbonyl compounds with the conjugated C=C and C=O bonds. The possible explanation is the conjugated "π" bond resulting in the electron delocalization of C=O bond, which reduces the repulsive interaction between the carbonyl oxygen and the oxygen of CO_2 and makes more CO_2 molecules congregating

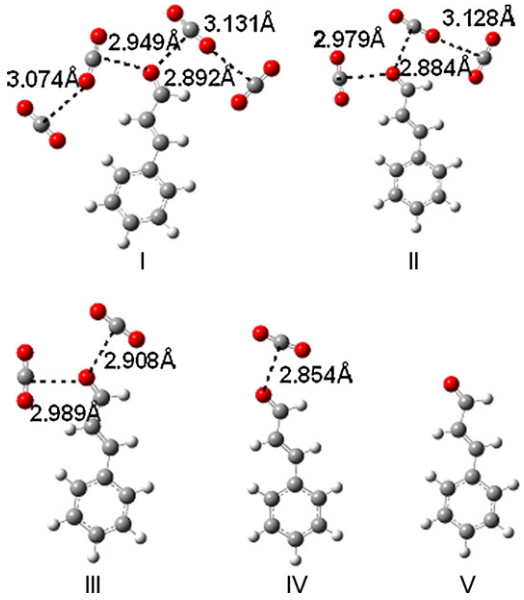

Fig. 6. Optimized geometries for the complex cinnamaldehyde–$(CO_2)_n$ (n = 0, 1, 2, 3, 4) at CO_2 pressure of 18 MPa.

Table 6
Change in carbonyl oxygen charge (Δq) and in the carbonyl bond length (ΔR) for carbonyl compounds at the CO_2 pressures 18 and 0 MPa and interaction energies ΔE_{cor} (kcal/mol) calculated using MP2/6-31+G* at the CO_2 pressures 18 MPa.

Molecular species	ΔE_{cor} (kcal/mol)[a]	Δq (me)	ΔR (mÅ)
Acetaldehyde	0	−8	0.86
Benzaldehyde	−1.918	−24	2.51
Acetone	−4.942	−37	3.79
Crotonaldehyde	−8.652	−61	7.75
Cinnamaldehyde	−9.151	−57	8.02

[a] ΔE_{cor} is the interaction energy corrected from BSSE.

around C=O. The changes in carbonyl oxygen charge and bond length of C=O of carbonyl compounds at a CO_2 pressure of 18 MPa are also calculated (Table 6). We find that the changes in the oxygen charge and C=O bond length are in an order of acetaldehyde < benzaldehyde < acetone < crotonaldehyde < cinnamaldehyde. This is the same to the order of the molecular interaction energies (ΔE_{cor}). Therefore, the reactivity of C=O bond is enhanced through the interaction with CO_2, which makes C=O bond more active because the longer C=O bond length is easier to break, and the higher oxygen charge in C=O is more favorable for electrophilic attack. This conclusion is in good agreement with the results from the previous experimental studies [11,19], in which the conversion of crotonaldehyde and cinnamaldehyde are enhanced significantly in $scCO_2$ compared with that of benzaldehyde, although its C=O bond is also more active at high pressure. These can also be identified by using the softness of C=O bond in the following.

4.4. Calculation of local softness for crotonaldehyde and benzaldehyde in $scCO_2$

In the past two decades, the reactivity descriptors such as local hardness [42,48] local softness [42], Fukui function [41], etc. have emerged as powerful tools in predicting the reactive sites of molecules. It is well known that the reactivity of molecules depends on the solvent environment. Chatterjee et al. used the local softness to successfully explain the effect of $scCO_2$ and organic solvent on selective hydrogenation of conjugated and isolated C=C of citral [49].

In this work, in order to explain the effects of CO_2 on crotonaldehyde and benzaldehyde, the local softness s_k^+ was calculated by the cluster–continuum model. The results are given in Table 7. For crotonaldehyde, the local softness s_k^+ values of C3 (for the numbering of molecule, see Fig. 7) were always higher than the other carbons in the range of pressure of 0–18 MPa, meaning that C3 is much easier to be attacked in nucleophilic reaction. As CO_2 pressure is increased from 0 to 18 MPa, the values of C3 change from 0.703 to 0.804 (with an increment Δ of 0.101). For C1, the values change from 0.478 to 0.671 (Δ 0.193). This indicates that the pressure change has significant effect on the reactivity of C=O bond compared with that of C=C bond. For benzaldehyde, the values of C(benz) changed from 0.481 to 0.581 (Δ 0.100), in which this increment is smaller than 0.193 of C1 in crotonaldehyde. This suggested that $scCO_2$ could improve the reactivity of C=O significantly in crotonaldehyde compared with that in benzaldehyde. This is consistent with experiment data for hydrogenation of crotonaldehyde and benzaldehyde [8,19].

Table 7
The local softness (s^+) of different atoms for crotonaldehyde and benzaldehyde.

Atom species	Pressure (MPa)					
	0	6	8.5	10	16	18
Crotonaldehyde[a]						
C3	0.703	0.701	0.719	0.735	0.773	0.804
C2	0.196	0.165	0.166	0.170	0.171	0.167
C1	0.478	0.565	0.584	0.599	0.639	0.671
O5	0.522	0.536	0.543	0.553	0.576	0.628
Benzaldehyde						
C(benz)[b]	0.481	0.516	0.529	0.543	0.578	0.581
O(benz)[c]	0.460	0.482	0.490	0.500	0.522	0.525

[a] The atom marked crotonaldehyde is shown in Fig. 7.
[b] C(benz) is the carbon of the carbonyl group of benzaldehyde.
[c] O(benz) is the oxygen of the carbonyl group of benzaldehyde.

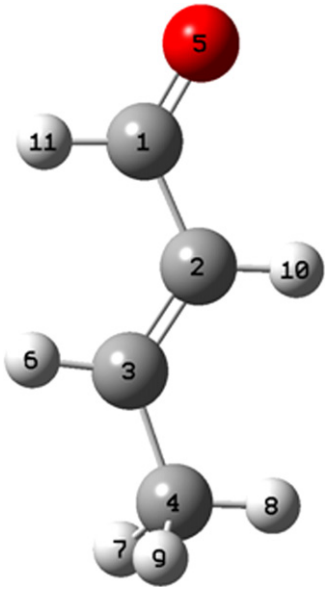

Fig. 7. Atoms numbered in crotonaldehyde.

5. Conclusions

In situ high-pressure FTIR experiments have been performed for several carbonyl compounds diluted in supercritical CO_2 at constant temperature $T = 50\,^{\circ}C$ at CO_2 pressures varying from 6 to 22 MPa. Then, the density functional method combined with vibrational spectroscopy has been carried out to study the interactions between CO_2 and carbonyl compounds (acetone, acetaldehyde, benzaldehyde, crotonaldehyde, cinnamaldehyde) at different supercritical CO_2 pressures. For acetone, the most suitable conformer is acetone–$(CO_2)_2$, in particular at elevated pressures 8.5–22 MPa. Benzaldehyde prefers to interact with one CO_2. For crotonaldehyde, due to the conjugated "π" bond, with the increase of the pressure, more and more CO_2 interact with crotonaldehyde. For the relatively large molecule of cinnamaldehyde, which contains both benzene ring and ethylene conjugating with carbonyl group, more than four CO_2 molecules interact with cinnamaldehyde. For acetaldehyde, the calculated frequency shift for the molecule itself (i.e., without interaction with CO_2) gives good agreement compared with the experimental result.

The interacting energies (ΔE_{cor}) at 18 MPa are in an order of acetaldehyde < benzaldehyde < acetone < crotonaldehyde < cinnamaldehyde, which is the same order as the change of the carbonyl oxygen charge and the carbonyl bond length. The reactivity of C=O bond was enhanced as a result of the interaction with CO_2, which makes C=O bond more activated. Finally, to explain CO_2 solvent effect on hydrogenation of crotonaldehyde and benzaldehyde, the values of the local softness have been calculated. The change of CO_2 pressure has a significant effect on the reactivity of C=O bond compared with that of C=C bond for crotonaldehyde. C=O bond in crotonaldehyde becomes more reactive compared with that in benzaldehyde in $scCO_2$, in agreement with the experiment observation.

Acknowledgments

The authors gratefully acknowledge to the financial support from the NSFC 20573104 and the One Hundred Talent Program of CAS.

Appendix A. Supplementary data

Supplementary data associated with this article can be found, in the online version, at doi:10.1016/j.supflu.2010.03.002.

References

[1] R. Marr, T. Gamse, Use of supercritical fluids for different processes including new developments—a review, Chem. Eng. Proc. 39 (2000) 19–28.
[2] A. Baiker, Supercritical fluids in heterogeneous catalysis, Chem. Rev. 99 (1999) 453–474.
[3] Y. Zhu, X.H. Lu, J. Zhou, Y.R. Wang, J. Shi, Prediction of diffusion coefficients for gas, liquid and supercritical fluid: application to pure real fluids and infinite dilute binary solutions based on the simulation of Lennard–Jones fluid, Fluid Phase Equilib. 194–197 (2002) 1141–1159.
[4] S. Fujita, S. Akihara, F.Y. Zhao, R.X. Liu, M. Hasegawa, M. Arai, Selective hydrogenation of cinnamaldehyde using ruthenium–phosphine complex catalysts with multiphase reaction systems in and under pressurized carbon dioxide: significance of pressurization and interfaces for the control of selectivity, J. Catal. 236 (2005) 101–111.
[5] F.Y. Zhao, S. Fujita, J.M. Sun, Y. Ikushima, M. Arai, Carbon dioxide-expanded liquid substrate phase: an effective medium for selective hydrogenation of cinnamaldehyde to cinnamyl alcohol, Chem. Commun. 20 (2004) 2326–2327.
[6] F.Y. Zhao, Y. Ikushima, M. Chatterjee, O. Sato, M. Arai, Hydrogenation of an alpha,beta-unsaturated aldehyde catalyzed with ruthenium complexes with different fluorinated phosphine compounds in supercritical carbon dioxide and conventional organic solvents, J. Supercrit. Fluids 27 (2003) 65–72.
[7] N. Hiyoshi, R. Miura, C.V. Rode, O. Sato, M. Shirai, Enhanced selectivity to decalin in naphthalene hydrogenation under supercritical carbon dioxide, Chem. Lett. 34 (2005) 424–425.
[8] S. Ichikawa, M. Tada, Y. Iwasawa, T. Ikariya, The role of carbon dioxide in chemoselective hydrogenation of halonitroaromatics over supported noble metal catalysts in supercritical carbon dioxide, Chem. Commun. 8 (2005) 924–926.
[9] I. Kani, R. Flores, J.P. Fackler, A. Akgerman, Hydroformylation of styrene in supercritical carbon dioxide with fluoroacrylate polymer supported rhodium catalysts, J. Supercrit. Fluids 31 (2004) 287–294.
[10] P. Stephenson, P. Licence, S.K. Ross, M. Poliakoff, Continuous catalytic asymmetric hydrogenation in supercritical CO_2, Green Chem. 6 (2004) 521–523.
[11] F.Y. Zhao, S. Fujita, S. Akihara, M. Arai, Hydrogenation of benzaldehyde and cinnamaldehyde in compressed CO_2 medium with a Pt/C catalyst: a study on molecular interactions and pressure effects, J. Phys. Chem. A 109 (2005) 4419–4424.
[12] F.Y. Zhao, S. Fujita, J.M. Sun, Y. Ikushima, M. Arai, Hydrogenation of nitro compounds with supported platinum catalyst in supercritical carbon dioxide, Catal. Today 98 (2004) 523–528.
[13] F.Y. Zhao, R. Zhang, M. Chatterjee, Y. Ikushima, M. Arai, Hydrogenation of nitrobenzene with supported transition metal catalysts in supercritical carbon dioxide, Adv. Synth. Catal. 346 (2004) 661–668.
[14] F.Y. Zhao, Y. Ikushima, M. Shirai, T. Ebina, M. Arai, Influence of electronic state and dispersion of platinum particles on the conversion and selectivity of hydrogenation of an α,β-unsaturated aldehyde in supercritical carbon dioxide, J. Mol. Catal. A: Chem. 180 (2002) 259–265.
[15] F. Zhao, Y. Ikushima, M. Arai, Hydrogenation of nitrobenzene with supported platinum catalysts in supercritical carbon dioxide: effects of pressure, solvent, and metal particle size, J. Catal. 224 (2004) 479–483.
[16] M. Chatterjee, F.Y. Zhao, Y. Ikushima, Hydrogenation of citral using monometallic Pt and bimetallic Pt–Ru catalysts on a mesoporous support in supercritical carbon dioxide medium, Adv. Synth. Catal. 346 (2004) 459–466.
[17] M. Chatterjee, F.Y. Zhao, Y. Ikushima, Effect of synthesis variables on the hydrogenation of cinnamaldehyde over Pt-MCM-48 in supercritical CO_2 medium, Appl. Catal. A: Gen. 262 (2004) 93–100.
[18] M. Chatterjee, Y. Ikushima, F.Y. Zhao, Completely selective hydrogenation of trans-cinnamaldehyde to cinnamyl alcohol promoted by a Ru–Pt bimetallic catalyst supported on MCM-48 in supercritical carbon dioxide, New J. Chem. 27 (2003) 510–513.
[19] F. Zhao, Y. Ikushima, M. Chatterjee, M. Shirai, M. Arai, An effective and recyclable catalyst for hydrogenation of alpha,beta-unsaturated aldehydes into saturated aldehydes in supercritical carbon dioxide, Green Chem. 5 (2003) 76–79.
[20] M. Chatterjee, Y. Ikushima, F.Y. Zhao, Highly efficient hydrogenation of cinnamaldehyde catalyzed by Pt-MCM-48 in supercritical carbon dioxide, Catal. Lett. 82 (2002) 141–144.
[21] R.X. Liu, F.Y. Zhao, S. Fujita, M. Arai, Selective hydrogenation of citral with transition metal complexes in supercritical carbon dioxide, Appl. Catal. A: Gen. 316 (2007) 127–133.
[22] M.R. Nelson, R.F. Borkman, Ab initio calculations on CO_2 binding to carbonyl groups, J. Phys. Chem. A 102 (1998) 7860–7863.
[23] M.A. Blatchford, P. Raveendran, S.L. Wallen, Spectroscopic studies of model carbonyl compounds in CO_2: evidence for cooperative C–H···O interactions, J. Phys. Chem. A 107 (2003) 10311–10323.
[24] P. Lalanne, T. Tassaing, Y. Danten, F. Cansell, S.C. Tucker, M. Besnard, CO_2–ethanol interaction studied by vibrational spectroscopy in supercritical CO_2, J. Phys. Chem. A 108 (2004) 2617–2624.
[25] C. Cappelli, B. Mennucci, C.O. da Silva, J. Tomasi, Refinements on solvation continuum models: hydrogen-bond effects on the OH stretch in liquid water and methanol, J. Chem. Phys. 112 (2000) 5382–5392.
[26] M.J. Frisch, G.W. Trucks, H.B. Schlegel, G.E. Scuseria, M.A. Robb, J.R. Cheeseman, J.A. Montgomery Jr., T. Vreven, K.N. Kudin, J.C. Burant, J.M. Millam, S.S. Iyengar, J. Tomasi, V. Barone, B. Mennucci, M. Cossi, G. Scalmani, N. Rega, G.A. Petersson, H. Nakatsuji, M. Hada, M. Ehara, K. Toyota, R. Fukuda, J. Hasegawa, M. Ishida, T. Nakajima, Y. Honda, O. Kitao, H. Nakai, M. Klene, X. Li, J.E. Knox, H.P. Hratchian, J.B. Cross, C. Adamo, J. Jaramillo, R. Gomperts, R.E. Stratmann, O. Yazyev, A.J. Austin, R. Cammi, C. Pomelli, J.W. Ochterski, P.Y. Ayala, K. Morokuma, G.A. Voth, P. Salvador, J.J. Dannenberg, V.G. Zakrzewski, S. Dapprich, A.D. Daniels, M.C. Strain, O. Farkas, D.K. Malick, A.D. Rabuck, K. Raghavachari, J.B. Foresman, J.V. Ortiz, Q. Cui, A.G. Baboul, S. Clifford, J. Cioslowski, B.B. Stefanov, G. Liu, A. Liashenko, P. Piskorz, I. Komaromi, R.L. Martin, D.J. Fox, T. Keith, M.A. Al-Laham, C.Y. Peng, A. Nanayakkara, M. Challacombe, P.M.W. Gill, B. Johnson, W. Chen, M.W. Wong, C. González, J.A. Pople, Gaussian 03, Revision B.02, Gaussian, Inc., Pittsburgh, PA, 2003.
[27] A.D. Becke, Density-functional exchange-energy approximation with correct asymptotic behavior, Phys. Rev. A 38 (1988) 3098–3100.
[28] C. Lee, W. Yang, R.G. Parr, Development of the Colle–Salvetti correlation-energy formula into a functional of the electron density, Phys. Rev. B 37 (1988) 785–789.
[29] A.D. Becke, Density-functional thermochemistry. III. The role of exact exchange, J. Chem. Phys. 98 (1993) 5648–5652.
[30] S.F. Boys, F. Bernardi, The calculation of small molecular interaction by the differences of separate total energies: some procedures with reduced errors, Mol. Phys. 19 (1970) 553–566.
[31] S. Miertuš, E. Scrocco, J. Tomasi, Electrostatic interaction of a solute with a continuum. A direct utilization of ab initio molecular potentials for the prevision of solvent effects, Chem. Phys. 55 (1981) 117–129.
[32] R. Cammi, J. Tomasi, Remarks on the use of the apparent surface charges (ASC) methods in solvation problems: Iterative versus matrix-inversion procedures and the renormalization of the apparent charges, J. Comp. Chem. 16 (1995) 1449–1458.
[33] J. Tomasi, M. Persico, Molecular interactions in solution: an overview of methods based on continuous distributions of the solvent, Chem. Rev. 94 (1994) 2027–2094.
[34] K. Miaskiewicz, Z. Kecki, Vibrational frequencies and force-constants of N_2O_4 in complexes with molecules of different solvents determined by Raman-spectra and ab initio calculation, J. Sol. Chem. 19 (1990) 465–471.
[35] Josefredo R. Pliego Jr., José M. Riveros, The cluster–continuum model for the calculation of the solvation free energy of ionic species, J. Phys. Chem. A 105 (2001) 7241–7247.
[36] T. Moriyoshi, T. Kita, Y. Uosaki, Ber Bunsenges, Static relative permittivity of carbon dioxide and nitrous oxide up to 30 MPa, Phys. Chem. 97 (1993) 589–596.
[37] D. Ben-Amotz, D.R. Herschbach, Estimation of effective diameters for molecular fluids, J. Phys. Chem. 94 (1990) 1038–1047.
[38] E.D. Glendening, J.K. Badenhoop, A.E. Reed, J.E. Carpenter, F. Weihold, NBO 3.1, Theoretical Chemistry Institute, University of Wisconsin, Madison, WI, 1996.
[39] R.G. Pearson, Hard and soft acids and bases, J. Am. Chem. Soc. 83 (1963) 3533–3539.
[40] R.G. Pearson, Acids and bases, Science 151 (1966) 172–177.
[41] R.G. Parr, W. Yang, Density functional approach to the frontier-electron theory of chemical reactivity, J. Am. Chem. Soc. 106 (1984) 4049–4050.
[42] W. Yang, R.G. Parr, Hardness, softness, and the Fukui function in the electronic theory of metals and catalysis, Proc. Natl. Acad. Sci. U.S.A. 82 (1985) 6723–6726.
[43] P. Raveendran, S.L. Wallen, Cooperative, C–H···O hydrogen bonding in CO_2–Lewis base complexes: implications for solvation in supercritical CO_2, J. Am. Chem. Soc. 124 (2002) 12590–12599.
[44] S.C. Tucker, Solvent density inhomogeneities in supercritical fluids, Chem. Rev. 99 (1999) 391–418.
[45] S.A. Egorov, J.L. Skinner, Vibrational line shifts in supercritical fluids, J. Phys. Chem. A 104 (2000) 483–489.
[46] Y. Danten, T. Tassaing, M. Besnard, Vibrational spectra of CO_2–electron donor–acceptor complexes from ab initio, J. Phys. Chem. A 106 (2002) 11831–11840.
[47] M. Besnard, M.I. Cabaco, S. Longelin, T. Tassaing, Y. Danten, Raman investigation of the CO_2 complex formation in CO_2–acetone mixtures, J. Phys. Chem. A 111 (2007) 13371–13379.
[48] S.K. Ghosh, M. Berkowitz, A classical fluid-like approach to the density-functional formalism of many-electron systems, J. Chem. Phys. 83 (1985) 2976–2983.
[49] A. Chatterjee, M. Chatterjee, Y. Ikushima, F. Mizukami, The role of solvent on selective hydrogenation of conjugated and isolated C=C of citral (3,7-dimethyl 2,6-octadienal)—a self-consistent reaction field study, Chem. Phys. Lett. 395 (2004) 143–149.